Research Square

Preprints are preliminary reports that have not undergone peer review.
They should not be considered conclusive, used to inform clinical practice,
or referenced by the media as validated information.

# A Scheme-Stage Aspect-Ratio Criterion for Determining When Pedestals Require Anchor Reinforcement in Elevated Tank Towers

**Eghosasere Oluwaseyi Rowland-Lato**

eghosa.rowland-lato@uniport.edu.ng

University of Port Harcourt

**Research Article**

**Keywords:** elevated water tank, uplift, concrete breakout, pedestal, anchor reinforcement, skew wind, EN 1992-4

**Posted Date:** October 29th, 2026

**DOI:** https://doi.org/10.21203/rs.3.rs-11244121/v1

**License:** This work is licensed under a Creative Commons Attribution 4.0 International License.
Read Full License

**Additional Declarations:** No competing interests reported.

# A Scheme-Stage Aspect-Ratio Criterion for Determining When Pedestals Require Anchor Reinforcement in Elevated Tank Towers

**Eghosasere Oluwaseyi Rowland-Lato**
Department of Civil Engineering, University of Port Harcourt, Rivers State, Nigeria
E-mail: eghosa.rowland-lato@uniport.edu.ng · ORCID: 0000-0001-7289-0530

## Highlights

- Stanchion uplift equals the factored stabilising load per stanchion times ($\eta - 1$).
- Pedestal breakout resistance is capped independently of bolt size and grade.
- Concrete-only anchorage ends at $(H/B)_2 = (H/B)_1(1 + \rho_a)$.
- Criterion matched 3D frame classification for 297 of 300 random towers.
- At $v_b = 40$ m/s, typical towers on 700 mm pedestals need anchor reinforcement.

## Abstract

Drained elevated steel tanks under skew wind can place windward stanchion bases in tension, and that tension must pass through headed bolts into concrete pedestals whose plan size limits the concrete breakout resistance. Current design practice discovers whether anchor reinforcement is needed only after the tower has been analysed and the pedestals sized. This paper derives a criterion that makes the decision at scheme stage. Rigid-group equilibrium with EN 1990 and EN 1991-1-4 actions shows that the design uplift equals the factored stabilising load per stanchion multiplied by $(\eta - 1)$, where $\eta$ is a dimensionless demand ratio. The EN 1992-4 narrow-member rule caps the breakout resistance of any symmetric bolt group in a square pedestal of side a at $(\sqrt{6}/9)k_1\sqrt{f_{ck}}\, a^{1.5}/\gamma_{Mc}$, independent of bolt diameter and grade. Combining the two gives the base aspect ratio at which concrete-only anchorage ends, $(H/B)_2 = (H/B)_1(1 + \rho_a)$, where $(H/B)_1$ is the onset of uplift and $\rho_a$ is the ratio of total pedestal resistance to factored stabilising load. The criterion was checked against a three-dimensional frame model over 108 configurations and classified 297 of 300 randomly generated towers in the same region as frame analysis combined with EN 1992-4; an 8% demand allowance for multi-leg towers with corner-supported tanks removed the single unconservative case. At a basic wind velocity of 40 m/s, $(H/B)_2$ was 1.37 to 2.17 for a 15 m tower with a 100 $m^3$ tank

on 700 mm C30/37 pedestals, well below the aspect ratios of built towers, so anchor reinforcement should be planned from the outset.

**Keywords:** elevated water tank; uplift; concrete breakout; pedestal; anchor reinforcement; skew wind; EN 1992-4

## *1. INTRODUCTION*

Elevated water tanks supported on steel lattice or braced-frame towers are common in municipal, institutional and industrial water supply. Where seismic actions are small, their lateral design is governed by wind. Steel and glass-reinforced plastic panel tanks weigh only a fraction of the water they hold, so the stabilising load available to resist overturning is smallest when the tank is drained, which is also the condition in which the wind area is unchanged. Under wind at skew to the stanchion grid, the windward corner stanchion can then be placed in tension.

The tension must travel from the base plate through cast-in headed bolts into a concrete pedestal. Pedestals are usually sized from the base plate, typically 600 to 900 mm square, long before the anchorage is checked. In a member this narrow, the idealised breakout body of a deep anchor meets the side faces, and the concrete breakout resistance given by EN 1992-4 [1] and ACI 318-19 [2] stops increasing with embedment. When the design uplift exceeds that bounded resistance, the anchorage must be carried by anchor reinforcement, which changes the embedment, the reinforcement layout and often the pedestal size. In current practice this is found only after the tower analysis, the pedestal geometry and the bolt layout have been fixed.

The codes do not index this transition to the geometry of the supported structure. EN 1990 [3] and EN 1991-1-4 [4] deliver the load combination and the wind actions; EN 1993-3-1 [5] treats base reactions as analysis output; EN 1992-4 [1], ACI 318-19 [2] and base-plate guidance [6] check a given anchor force against a given member. No criterion was found in

the literature reviewed that states, in terms of quantities available before analysis, the base aspect ratio above which a pedestal can no longer rely on concrete breakout.

This paper derives such a criterion and tests it. Its contributions are:

1. a dimensionless demand ratio $\eta$, with the identity $\eta = (N_c + N_t)/(N_c - N_t)$ that recovers it from any two reported extreme reactions;
2. a bound on the EN 1992-4 breakout resistance of symmetric bolt groups in square pedestals that is independent of bolt size and grade;
3. the transition criterion $(H/B)_2 = (H/B)_1(1 + \rho_a)$, verified against a three-dimensional frame model and a 300-tower Monte Carlo sample, with a worked design procedure.

The criterion is a rearrangement of existing code provisions, not a new resistance model. Its value lies in when it can be applied: at scheme stage, from the tank, tower and pedestal dimensions alone.

## *2. BACKGROUND*

### *2.1 Wind Actions and Base Reactions of Lattice Towers*

Wind-tunnel and aeroelastic studies of lattice towers show that code values of the quantities entering the base reactions may be low. Zhou et al. [7] found that standards underestimate the skewed wind load factor of tower bodies by at least 10%, and D. Zhang et al. [8] and Tang et al. [9] reported that skewed load factors vary with geometry in ways the codes do not capture. W. Zhang et al. [10] found the most unfavourable attack angles away from 45°. Jeddi et al. [11] measured drag coefficients and gust response factors up to 12% and 13% above recommended values, and Azzi et al. [12] found a resonant contribution of up to 18% of the peak response of a self-supported lattice tower. These studies end at the member forces or base reactions of specific towers; none relates the reactions to the anchorage resistance of the foundation.

The tank literature addresses a different part of the problem. For ground-supported tanks, the empty condition governs uplift of the bottom plate [13] and shell buckling under wind [14]. For elevated tanks, research has concentrated on seismic response, where the full tank is

usually critical [15,16], on isolation [17], and on the wind reliability of heavy concrete reservoirs [18]. The empty-tank uplift of light steel-tank towers has received little attention.

### *2.2 Concrete Breakout in Narrow Members*

The breakout model of EN 1992-4 and ACI 318-19 derives from the concrete capacity design (CCD) method [19,20], in which the resistance of a single anchor grows with $h_{ef}^{1.5}$ and is reduced by the ratio of projected areas where edges or neighbouring anchors truncate the failure body. For anchors close to three or more edges, both codes replace $h_{ef}$ by a modified embedment $h'_{ef}$ fixed by the largest edge distance and the largest spacing [1,2]. Stehle and Sharma [21] showed that this narrow-member approach is conservative, and Karmokar et al. [22] noted that deep anchors lie outside the range on which the CCD method was calibrated. Qian et al. [23] observed that deep anchor groups in members of limited width can fail by splitting, and Bokor et al. [24] and Sharma and Eligehausen [25] showed that the CCD method presupposes a linear distribution of anchor forces, which a flexible base plate may not provide.

### *2.3 Column Bases and Anchor Reinforcement*

For column bases, the concrete breakout check is performed once the anchor forces are known [6,26,27]. Grilli and Kanvinde [26] found the CCD method accurate for embedded column-base anchor groups, with a mean test-to-prediction ratio of 0.99. Kishiki et al. [27] found that column reinforcement engaged only after concrete breakout, whereas Worsfold and Moehle [28] proposed an additive design for column-foundation connections. Tests on anchor reinforcement [29–32] show that it can replace the concrete contribution, although Petersen et al. [29] found that code-conforming reinforcement did not always ensure steel failure of the anchor. What these studies share is the order of operations: the anchor force comes first and the anchorage check follows. The present criterion reverses that order for towers.

## 3. FORMULATION

### 3.1 Scope and Assumptions

The tower is prismatic with vertical stanchions on a regular $n_x$ by $n_y$ grid of weak-axis width B and height H to the tank floor. The tank is carried on a top grillage. Each stanchion is anchored by a symmetric group of cast-in headed bolts in its own square pedestal of side a, and the pedestals bear on a common raft or on foundations of uniform stiffness. The governing combination for uplift is the drained tank under skew wind. Fig. 1 defines the geometry, and Table 1 lists the assumptions and where each is tested.

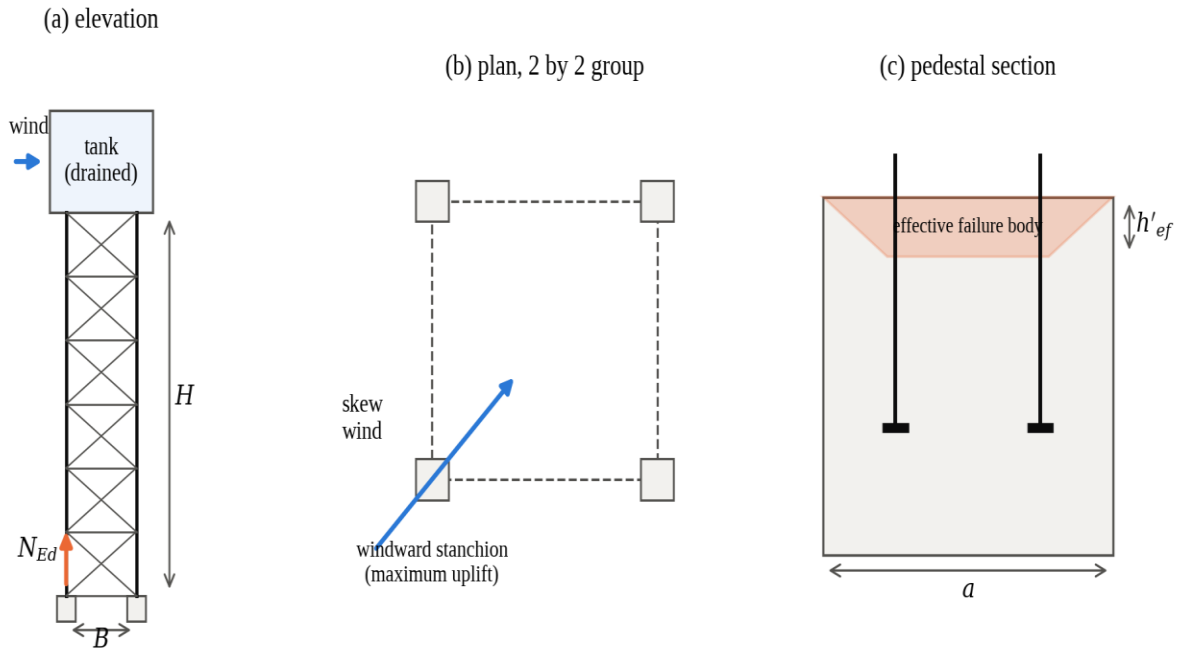


Fig. 1. Definitions: (a) tower elevation with the windward stanchion in tension; (b) plan of a 2 by 2 group under skew wind; (c) pedestal of side a with the effective breakout body limited to $h'_{ef}$ by the narrow-member rule.

Table 1. Principal assumptions.

| Assumption | Basis | Tested in |
|---|---|---|
| Base reactions follow a rigid-group (linear) distribution | Stiff grillage and uniform supports | Section 5.2, frame model |
| Drained tank with skew wind governs uplift | Minimum stabilising load, unchanged wind area | Section 6.3 |
| Skew wind: κ/2 of each orthogonal moment, κ = 1.70 | Design convention of the case study | Section 5.1, sensitivity |
| Breakout resistance to EN 1992-4 with the narrow-member rule, cracked concrete | Current European standard | Section 6.1, ACI 318-19 comparison |
| Pedestal bars and links not credited | Not detailed as anchor reinforcement | Section 6.3 |
| Wind actions to EN 1991-1-4, terrain category II, $c_s\,c_d = 1$ | Quasi-static design value | Section 6.3 |

### *3.2 Design Reaction and Demand Ratio*

With stanchions at $(x_j, y_j)$ about the group centroid and orthogonal characteristic moments $M_y$ and $M_x$, the skew convention combines $\kappa/2$ of each. The design reaction at the windward corner is then

$$N_{Ed} = \gamma_Q \frac{\kappa}{2}\left(\frac{M_y}{W_x} + \frac{M_x}{W_y}\right) - \gamma_{G,inf} \frac{G_{empty}}{n} \tag{1}$$

where $W_x = \Sigma x_j^2/x_{max}$ and $W_y = \Sigma y_j^2/y_{max}$ are group moduli, n is the number of stanchions, $G_{empty}$ is the characteristic permanent load with the tank empty, and $\gamma_Q = 1.5$ and $\gamma_{G,inf} = 1.0$ are the partial factors of EN 1990 [3]. Defining the equivalent weak-axis moment $M_{eq} = (\kappa/2)(M_y + M_x W_x/W_y)$, the group coefficient $\lambda_g = W_x/(nB)$ and the uplift index $\Lambda = M_{eq}/(G_{empty} B)$, Eq. (1) becomes

$$N_{Ed} = \frac{\gamma_{G,inf} G_{empty}}{n}(\eta - 1), \qquad \eta = \frac{\gamma_Q \Lambda}{\gamma_{G,inf} \lambda_g} \tag{2}$$

The demand ratio $\eta$ is the factored overturning demand at the corner stanchion divided by the factored stabilising load per stanchion. Uplift begins at $\eta = 1$ and the design uplift is proportional to $\eta - 1$. For any two-row group, $\Sigma x_j^2 = n(B/2)^2$, so $\lambda_g = 1/2$ regardless of the number of stanchions per row; for a 3 by 3 group $\lambda_g = 1/3$.

### *3.3 Onset of uplift*

Writing the orthogonal moment as $M = \zeta F H$, where F is the total characteristic wind force and $\zeta$ the height of its resultant as a fraction of H, and $\omega = F/G_{empty}$ for the wind-to-weight ratio, the condition $\eta = 1$ for a square group ($M_{eq} = \kappa M$) gives the base aspect ratio at the onset of uplift:

$$\left(\frac{H}{B}\right)_1 = \frac{\gamma_{G,inf} \lambda_g}{\gamma_Q \kappa \zeta \omega} \tag{3}$$

When the lattice wind area does not depend on B, $\zeta$ and $\omega$ are independent of the base width and Eq. (3) is exact within the rigid-group idealisation. Because $\omega$ is proportional to $v_b^2$ and

inversely proportional to $G_{empty}$, $(H/B)_1$ falls with the square of the basic wind velocity and rises in proportion to the empty stabilising load.

### *3.4 Demand Ratio From Reported Reactions*

For a doubly symmetric group under one combination, the windward tension and the diagonally opposite compression are $N_t = X - g$ and $N_c = X + g$, with X the factored overturning term and $g = \gamma_{G,inf}\, G_{empty}/n$. Hence

$$\eta = \frac{N_c + N_t}{N_c - N_t} \tag{4}$$

so the demand ratio of any analysed tower can be recovered from its two extreme reactions. For the design case that motivated this study, $N_t$ = 566.3 kN and $N_c$ = 731.2 kN, giving $\eta$ = 7.87 and an implied factored stabilising load of 82.5 kN per stanchion.

### *3.5 Pedestal Ceiling*

Consider a symmetric group whose outer anchors span $g_x = g_y = g$ in a square pedestal of side a, with an embedment deep enough for the narrow-member rule of EN 1992-4 to govern. The outer edge distance is $c = (a - g)/2$ and the largest spacing is g, so $h'_{ef} = \max[(a - g)/3, g/3]$. For $g \le a/2$, the projected area reaches the pedestal faces, $A_{c,N} = a^2$, $A^0_{c,N} = 9h'^2_{ef}$ and $\psi_{s,N} = 1$, so that

$$N_{Rd,c}(g) = \frac{k_1\sqrt{f_{ck}}\, a^2}{3^{1.5}\,\gamma_{Mc}\sqrt{a-g}}, \qquad g \le a/2 \tag{5}$$

which increases with g. For $g \ge a/2$, $h'_{ef} = g/3$ and $\psi_{s,N} = 0.7 + 0.3(a - g)/g$, and the resistance decreases with g. The maximum occurs at g = a/2, with the bolts at the quarter points:

$$N_{Rd,c,max} = \varphi_g\, \frac{k_1\sqrt{f_{ck}}\, a^{1.5}}{\gamma_{Mc}}, \qquad \varphi_g = \frac{\sqrt{6}}{9} = 0.272 \tag{6}$$

For a single central anchor, $\varphi_g = 3^{-1.5} = 0.192$. With $k_1 = 8.9$ (cracked, cast-in) and $\gamma_{Mc} = 1.5$, Eq. (6) gives 163.8 kN for a 700 mm pedestal of C30/37 concrete. The ceiling contains no bolt property: once the embedment exceeds the plateau depth, no choice of bolt diameter,

grade or length raises the calculated breakout resistance. For practical bolt groups in such pedestals, the steel resistance exceeds the ceiling; four M24 grade 4.6 bolts have a design steel resistance of 282 kN, 1.7 times the ceiling, and pull-out resistances are larger still. The pedestal side required to carry a tension $N_{Ed}$ on concrete alone follows by inversion:

$$a_{req} = \left( \frac{\gamma_{Mc}\, N_{Ed}}{\varphi_g\, k_1 \sqrt{f_{ck}}} \right)^{2/3} \tag{7}$$

### *3.6 Transition Criterion*

Equating Eq. (2) with the resistance available at one stanchion gives the boundary between concrete-only anchorage and anchor reinforcement:

$$\eta = 1 + \rho_a, \qquad \rho_a = \frac{n\, N_{Rd,c}}{\gamma_{G,inf}\, G_{empty}} \tag{8}$$

The pedestal capacity ratio $\rho_a$ compares the breakout resistance of the whole foundation with the factored stabilising load; it contains no wind quantity. Because $\eta$ is proportional to H/B when height, tank and wind are fixed, the transition occurs at

$$\left(\frac{H}{B}\right)_2 = \left(\frac{H}{B}\right)_1 (1 + \rho_a) \tag{9}$$

and, substituting Eqs. (3) and (6), the largest aspect ratio for which a pedestal of side a can rely on concrete breakout is

$$\left(\frac{H}{B}\right)_{2,max} = \frac{\gamma_{G,inf}\, \lambda_g}{\gamma_Q\, \kappa\, \zeta\, \omega} \left[ 1 + \frac{n\, \varphi_g\, k_1 \sqrt{f_{ck}}\; a^{1.5}}{\gamma_{Mc}\, \gamma_{G,inf}\, G_{empty}} \right] \tag{10}$$

Equations (2) and (8) divide towers into three regions: Region I ($\eta \le 1$), in which every base is in compression; Region II ($1 < \eta \le 1 + \rho_a$), in which uplift occurs but concrete breakout suffices; and Region III ($\eta > 1 + \rho_a$), in which anchor reinforcement is required. Equation (9) shows that the width of Region II, measured by the ratio of the two thresholds, depends on $\rho_a$ alone.

### *3.7 Two Corollaries*

In Region III, EN 1992-4 replaces the breakout check by checks on the anchor reinforcement. If a bar is placed a horizontal distance e from the anchor and the idealised failure surface falls at 1 in 1.5 from the head, the bar crosses the surface at depth $h_{ef} - e/1.5$; developing an anchorage length $l_1$ above that crossing with top cover c requires

$$h_{ef} \geq l_1 + \frac{e}{1.5} + c \tag{11}$$

This geometric reading of the anchor-reinforcement model is not a clause of the code, but it shows that a Region III embedment is set by the reinforcement, not by the cone. Second, because $N_{Ed}$ is a difference of two terms, a proportional error in the wind moment is amplified in the uplift:

$$\frac{\Delta N_{Ed}}{N_{Ed}} = \frac{\eta}{\eta - 1} \frac{\Delta M}{M} \tag{12}$$

## *4. VERIFICATION METHODS*

### *4.1 Reference Towers and Actions*

Two reference towers were defined. RT-S has H = 15 m, B = 3.4 m (H/B = 4.41), a 2 by 2 stanchion grid and a 100 m³ steel panel tank, 5.0 by 5.0 by 4.0 m, with an empty tank ratio $\varepsilon_t$ (tank self-weight over water weight) of 0.1. RT-H is identical except that $\varepsilon_t = 0.6$. The tower self-weight was 4 kN/m and the grillage 25 kN. Wind actions followed EN 1991-1-4 [4] in terrain category II, with a tank force coefficient of 1.5 and lattice force coefficients from EN 1993-3-1 [5]. A basic wind velocity of 40 m/s was adopted as the reference value, representing a high-wind site; all thresholds are also reported from 20 to 45 m/s.

### *4.2 Three-Dimensional Frame Model*

A linear-elastic space-frame solver (direct stiffness method, six degrees of freedom per node) was written for the study. It generates braced towers with 2 by 2, 2 by 3 and 3 by 3 stanchion grids, circular hollow section legs, angle bracing, a top grillage whose stiffness was scaled by $k_g = 0.1$, 1 and 10, and a rigid tank linked either to the corner stanchions or to all stanchion

heads. The same factored loads were applied to the frame and to Eq. (1) for 108 combinations of layout, base fixity (pinned or fixed), grillage stiffness, tank support and wind direction. The solver was checked against closed-form cantilever deflections and, for the four-leg pinned tower, against Eq. (1) to $10^{-9}$ kN.

### *4.3 Monte Carlo Validation*

Three hundred towers were drawn from uniform distributions with a fixed seed: layout 2 by 2, 2 by 3 or 3 by 3; H = 8 to 25 m; H/B = 1 to 6; capacity 30 to 250 m³; $\varepsilon_t$ = 0.1 to 0.6; $v_b$ = 20 to 40 m/s; pedestal side 600, 700 or 900 mm; $f_{ck}$ = 25, 30 or 35 MPa. Each tower was classified into Region I, II or III twice: by the closed form, Eqs. (2) and (8), and by the frame model combined with the EN 1992-4 resistance of its pedestal. The derivations of Section 3 were also verified symbolically with a computer algebra system; every identity returned zero and the coefficient of Eq. (6) returned $\sqrt{6}/9$.

## *5. RESULTS*

### *5.1 Reference Towers and the Onset of Uplift*

For RT-S at $v_b$ = 40 m/s, the peak velocity pressure at the tank centroid (z = 17 m) was 2.70 kPa, the tank wind force 81.0 kN and the lattice force 47.5 kN, giving an orthogonal overturning moment of 1796 kN m with $\zeta$ = 0.932 and $\omega$ = 0.702. The drained skew combination produced a design uplift of 627.7 kN at the windward corner, 1.79 times the orthogonal value of 350.4 kN. Equation (3) gives $(H/B)_1 = 0.5/(1.5 \times 1.70 \times 0.932 \times 0.702) = 0.30$, equal to the root-finding solution; across 180 combinations of height, velocity, capacity and $\varepsilon_t$, the closed form agreed with root-finding to within $10^{-11}$%. For RT-H, $(H/B)_1 = 1.10$.

Table 2 reports the onset threshold and the transition threshold for the 15 m tower with a 100 m³ tank on 700 mm pedestals. At the reference wind speed, a tower carrying a light tank lifts at any aspect ratio above 0.30, far below the range of built towers, so uplift is the normal condition rather than a feature of slender towers. The ratio of the two thresholds is constant down each column, as Eq. (9) requires.

Table 2. Thresholds $(H/B)_1$ and $(H/B)_2$ for H = 15 m, V = 100 m³, a = 700 mm, C30/37 cracked, optimal 2 by 2 group.

| $v_b$ (m/s) | $\varepsilon_t$ = 0.1: $(H/B)_1$ | $(H/B)_2$ | $\varepsilon_t$ = 0.3: $(H/B)_1$ | $(H/B)_2$ | $\varepsilon_t$ = 0.6: $(H/B)_1$ | $(H/B)_2$ |
|---|---|---|---|---|---|---|
| 20 | 1.20 | 5.48 | 2.48 | 6.76 | 4.41 | 8.69 |
| 30 | 0.53 | 2.43 | 1.10 | 3.01 | 1.96 | 3.86 |
| 40 | 0.30 | 1.37 | 0.62 | 1.69 | 1.10 | 2.17 |
| 45 | 0.24 | 1.08 | 0.49 | 1.34 | 0.87 | 1.72 |
| $1 + \rho_a$ | 4.57 | | 2.72 | | 1.97 | |

The sensitivity of $(H/B)_1$ to its parameters is summarised in Table 3. Because $(H/B)_1$ is inversely proportional to the wind force, the percentage effects of the wind parameters are the same for both towers. Replacing the skew convention $\kappa = 1.70$ by $\sqrt{2}$, the value for a diagonal wind of the orthogonal magnitude, raises $(H/B)_1$ by 20.2%; the convention therefore carries a margin whose adequacy depends on the skew aerodynamics discussed in Section 2.1.

Table 3. Change in $(H/B)_1$ (%) for low and high parameter values; base values 0.30 (RT-S) and 1.10 (RT-H).

| Parameter (low / high) | RT-S low | RT-S high | RT-H low | RT-H high |
|---|---|---|---|---|
| Terrain category (III / I) | +32.0 | −13.4 | +32.0 | −13.4 |
| Basic wind velocity (36 / 44 m/s) | +23.5 | −17.4 | +23.5 | −17.4 |
| Empty tank ratio (−40% / +40%) | −21.4 | +21.4 | −35.0 | +35.0 |
| Skew factor (1.41 / 1.70) | +20.2 | 0.0 | +20.2 | 0.0 |
| Tank force coefficient (1.2 / 1.8) | +18.1 | −13.3 | +18.1 | −13.3 |
| Structural factor $c_s\,c_d$ (0.9 / 1.1) | +11.1 | −9.1 | +11.1 | −9.1 |
| Tower self-weight (3 / 5 kN/m) | −8.2 | +8.2 | −2.2 | +2.2 |

### *5.2 Accuracy of the Rigid-Group Idealisation*

Fig. 2 compares the maximum design uplift from Eq. (1) with the frame result under skew wind. For the four-leg tower with pinned bases the two agree exactly, as symmetry requires; with fixed bases Eq. (1) is conservative by 0.6% to 0.7% because the stanchion bases carry a small share of the overturning in bending. For six-leg and nine-leg towers whose tank bears on all stanchion heads, the difference stays within 1.0%. When the tank bears on the corner stanchions alone, the overturning is delivered preferentially to the corners and Eq. (1) underestimates the corner uplift by up to 7.9% with a flexible grillage ($k_g = 0.1$), falling to 2% to 3% with a stiff grillage. The rigid-group relationship is therefore not unconditionally

conservative, a finding that parallels the observation of Bokor et al. [24] at the scale of a single base plate.

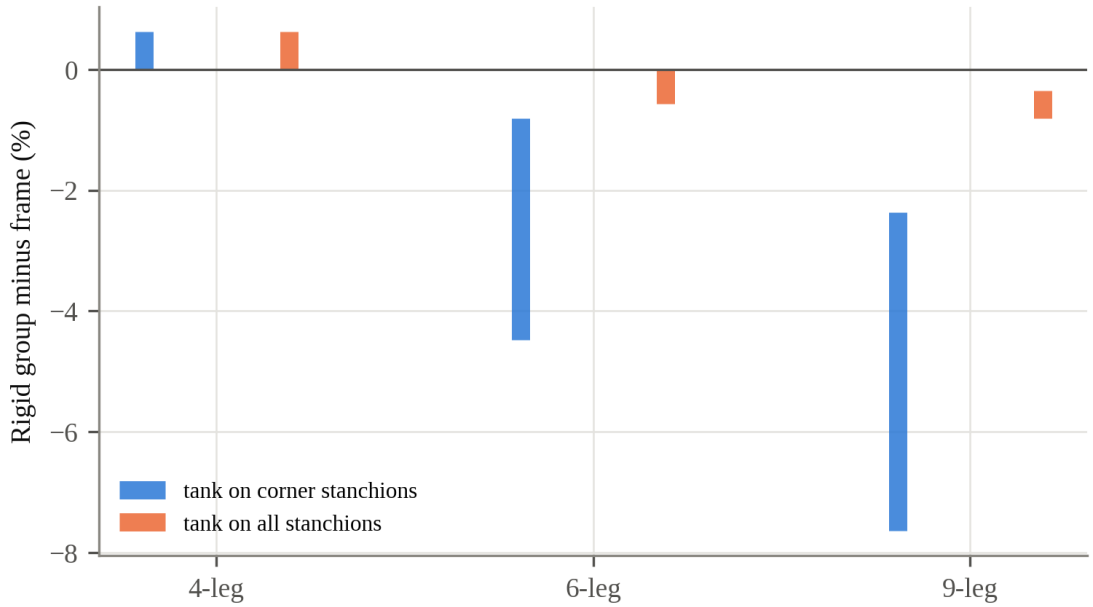


Fig. 2. Difference between the rigid-group (Eq. 1) and frame values of the maximum design uplift under skew wind, over grillage stiffness and base fixity, for three layouts and two tank-support arrangements.

### *5.3 Demand, Resistance and the Aspect Ratio*

Fig. 3 plots the design uplift of the 15 m tower against H/B together with the pedestal ceilings of Eq. (6). The uplift rises linearly with H/B once uplift begins, from 107 kN at H/B = 1.0 to 622 kN at H/B = 4.4 for $\varepsilon_t = 0.1$, whereas each ceiling is a horizontal line: 130, 163, 238 and 366 kN for pedestals of 600, 700, 900 and 1200 mm. The aspect ratio therefore acts only on the demand. The critical value $(H/B)_2$ is the abscissa at which the demand line meets the ceiling of the chosen pedestal. A slender tower does not weaken its pedestals; it asks more of the same resistance.

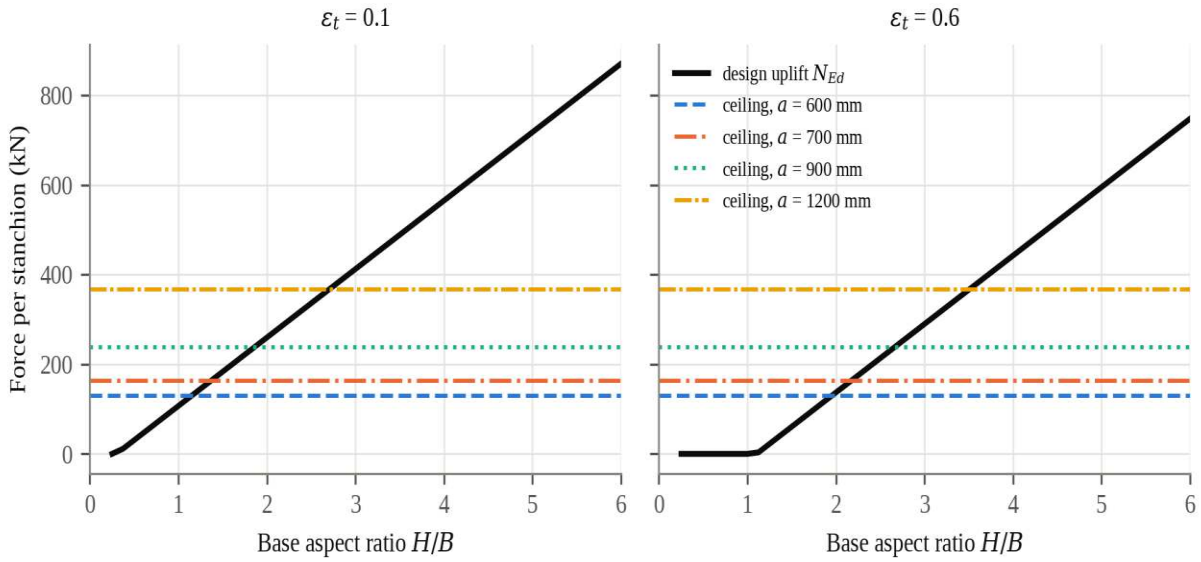


Fig. 3. Design uplift per stanchion against H/B for $\varepsilon_t$ = 0.1 and 0.6 (H = 15 m, V = 100 m³, $v_b$ = 40 m/s, skew wind) with the pedestal ceilings for optimally arranged 2 by 2 groups (C30/37, cracked). Intersections are the thresholds $(H/B)_2$.

### *5.4 Validation Against Frame Analysis*

Of the 300 random towers, frame analysis combined with EN 1992-4 placed 83 in Region I, 142 in Region II and 75 in Region III. The closed form placed 297 in the same region, an agreement of 99.0% (95% Wilson score interval 97.1% to 99.7%). Fig. 4 shows the sample in the plane of $\rho_a$ and $\eta$, and Table 4 lists the three disagreements. All three lie within 7.5% of a boundary. Two are conservative: the closed form placed the tower just above the onset of uplift while the frame found the corner stanchion marginally in compression. The third, a nine-leg tower with a corner-supported tank, was placed just below the Region III boundary by the closed form and just above it by the frame, reflecting the underestimate identified in Section 5.2. Increasing $\eta$ by 8% for multi-leg towers with corner-supported tanks removed this case without moving any correct classification to the unsafe side.

Table 4. Towers classified differently by the closed form and the frame analysis.

| Layout | $\eta$ | $1 + \rho_a$ | Frame $N_{Ed}$ (kN) | Rigid-group $N_{Ed}$ (kN) | $N_{Rd,c}$ (kN) | Closed form | Frame |
|---|---|---|---|---|---|---|---|
| 3 by 3 | 3.18 | 3.26 | 143.3 | 133.6 | 138.5 | II | III |
| 2 by 3 | 1.02 | 3.25 | −1.9 | 1.1 | 117.0 | II | I |
| 2 by 3 | 1.07 | 1.92 | −7.8 | 9.4 | 128.2 | II | I |

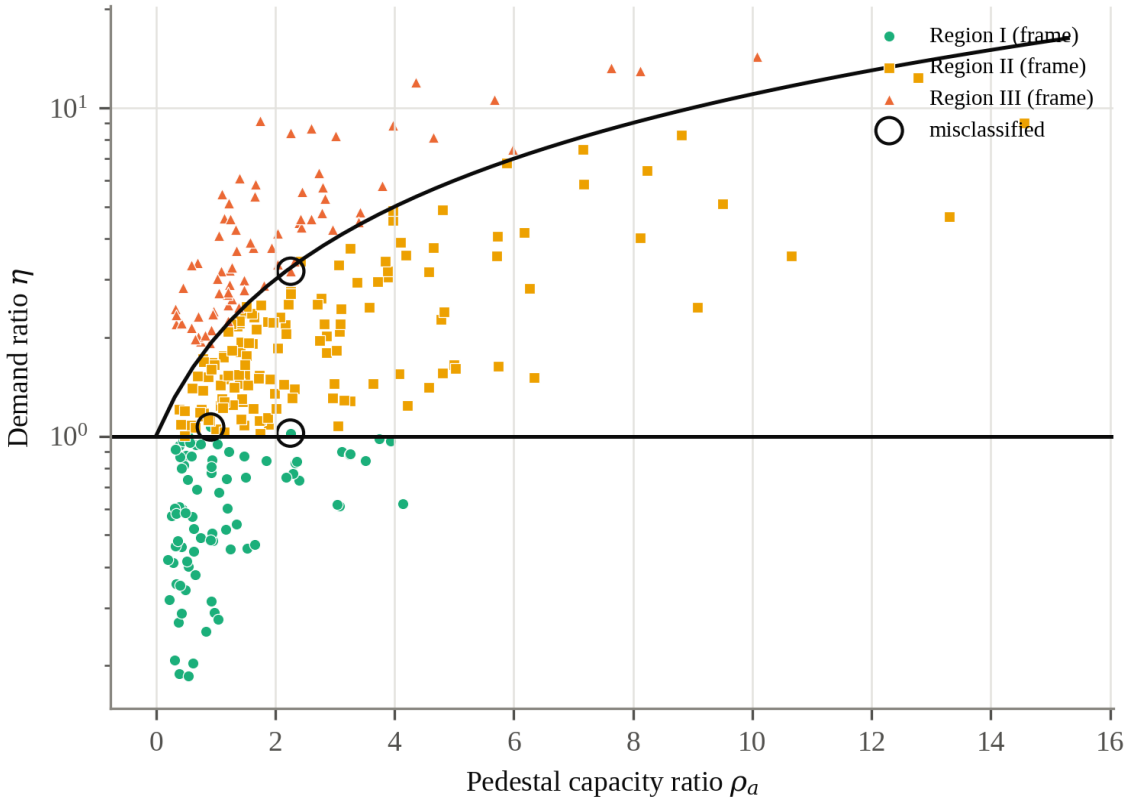


Fig. 4. Regime map in the plane of pedestal capacity ratio $\rho_a$ and demand ratio $\eta$ for 300 random towers classified by frame analysis with EN 1992-4. The lines $\eta = 1$ and $\eta = 1 + \rho_a$ are the region boundaries of Eqs. (2) and (8); circled points were classified differently by the closed form.

### *5.5 Design Maps*

For scheme design, Eq. (9) is more conveniently drawn in the plane of basic wind velocity and aspect ratio (Fig. 5). A tower below the black curve is in Region I, between it and the curve of its pedestal in Region II, and above that curve in Region III. For $\varepsilon_t = 0.3$ at 40 m/s, enlarging the pedestal from 600 to 700 and 900 mm raises $(H/B)_2$ from 1.47 to 1.69 and 2.18. Because the ceiling grows only with $a^{1.5}$, each further increment of $(H/B)_2$ costs a progressively larger pedestal, so enlargement helps towers near the boundary but not those well above it.

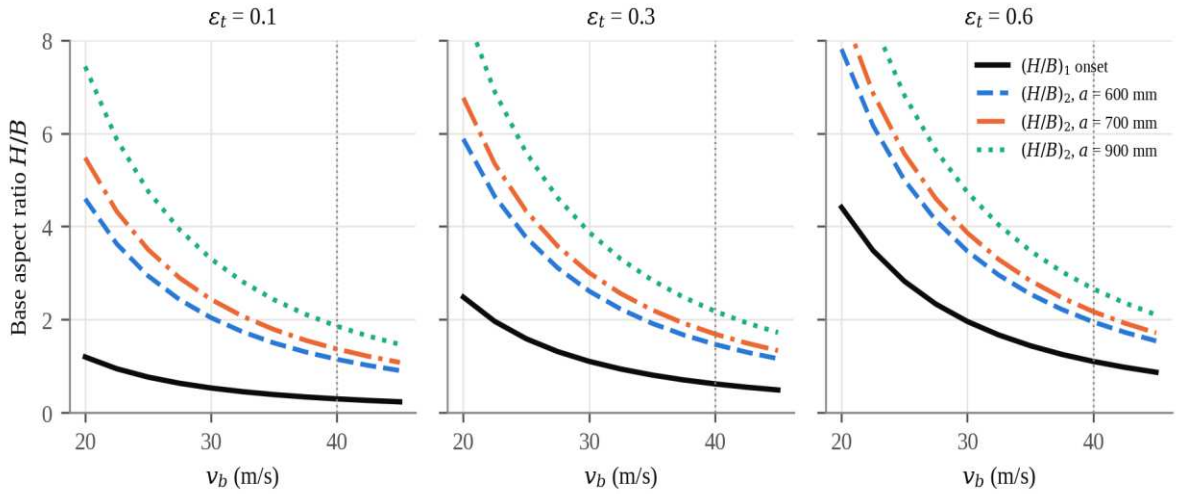


Fig. 5. Design maps for H = 15 m, V = 100 m³, C30/37 cracked, optimal 2 by 2 groups: onset threshold $(H/B)_1$ and transition thresholds $(H/B)_2$ for 600, 700 and 900 mm pedestals. The dotted line marks $v_b$ = 40 m/s.

### *5.6 Worked Application*

Table 5 applies the criterion to both reference towers. No structural analysis is needed. Both towers lie in Region III, but by different margins. For RT-S, $\eta$ = 14.71 is 3.2 times the boundary of 4.58; carrying the uplift on concrete alone would require 1714 mm pedestals or a base 10.9 m wide, so anchor reinforcement (eight H16 bars per stanchion in C30/37 with $f_{bd}$ = 3.04 MPa, hooked bars) with an embedment of about 510 mm is the practical response.

Table 5. Application of the criterion at $v_b$ = 40 m/s; a = 700 mm, C30/37 cracked, optimal 2 by 2 group.

| Step | Quantity | Source | RT-S ($\varepsilon_t$ = 0.1) | RT-H ($\varepsilon_t$ = 0.6) |
|---|---|---|---|---|
| 1 | Empty stabilising load $G_{empty}$ | Input | 183.1 kN | 673.6 kN |
| 2 | Orthogonal moment M | EN 1991-1-4 | 1796 kN m | 1796 kN m |
| 3 | Uplift index $\Lambda$ ($\kappa$ = 1.70) | Section 3.2 | 4.90 | 1.33 |
| 4 | Demand ratio $\eta$ | Eq. (2) | 14.71 | 4.00 |
| 5 | Design uplift $N_{Ed}$ | Eq. (2) | 627.7 kN | 505.1 kN |
| 6 | Pedestal ceiling $N_{Rd,c,max}$ | Eq. (6) | 163.8 kN | 163.8 kN |
| 7 | Pedestal capacity ratio $\rho_a$ | Eq. (8) | 3.58 | 0.97 |
| 8 | Region | $\eta$ vs 1 + $\rho_a$ | III | III |
| 9 | $(H/B)_1$; $(H/B)_2$ | Eqs. (3), (9) | 0.30; 1.37 | 1.10; 2.17 |
| 10 | Pedestal for concrete only | Eq. (7) | 1714 mm | 1483 mm |
| 11 | Base width for Region II | $H/(H/B)_2$ | 10.9 m | 6.9 m |
| 12 | Anchor reinforcement per stanchion | EN 1992-4 | 1444 mm², 8 H16 | 1162 mm², 6 H16 |
| 13 | Minimum embedment (e = 150, c = 50 mm) | Eq. (11) | 510 mm | 535 mm |
| 14 | Amplification $\eta/(\eta - 1)$ | Eq. (12) | 1.07 | 1.33 |

For RT-H, $\eta = 4.00$ is twice the boundary of 1.97. Pedestals of 900 or 1200 mm raise the boundary only to 2.42 and 3.18; the required side is 1483 mm. For the design case of Section 3.4, the same reasoning gives $\rho_a = 163.8/82.5 = 1.99$ per stanchion and a boundary of $\eta = 2.99$ against $\eta = 7.87$, confirming that its decision to carry the whole uplift in anchor reinforcement was required by the resistance model.

## *6. DISCUSSION*

### *6.1 Relation to the Codes*

The criterion reproduces the outcome of the EN 1992-4 check, within the errors of Section 5.4, because it is an exact reduction of the rigid-group calculation and of the code resistance. It differs from the code procedure in timing, not in result: the code answers whether a given anchorage is adequate for given forces, whereas the criterion tells the designer which kind of anchorage the tower will need before the forces are computed. Its form carries over to ACI 318-19 [2], whose three-edge rule has the same structure. For the optimal group in pedestals up to about 1.7 m, the ACI design ceiling is 1.18 times the EN value, the ratio of $10 \times 0.70$ to 8.9/1.5; with the EN demand retained, $(H/B)_2$ rises from 1.37 to 1.57 for RT-S and from 2.17 to 2.37 for RT-H. Towers between these values need anchor reinforcement under EN 1992-4 but not under ACI 318-19. A complete comparison would also use the ASCE/SEI 7-22 combination 0.9D + 1.0W [33], which enters the criterion only through the partial factors in $\eta$.

### *6.2 Why Light Tanks Behave Differently*

Equation (9) explains a pattern that is not obvious from analysis of individual towers. Light tanks have the lowest onset of uplift but the widest Region II, because their small stabilising load makes the foundation resistance large by comparison ($1 + \rho_a = 4.57$ for $\varepsilon_t = 0.1$ against 1.97 for $\varepsilon_t = 0.6$). For a light tank, enlarging the pedestals or improving the concrete buys a large increase in the admissible aspect ratio; for a heavy tank the same change buys little. At

40 m/s, however, even the wide Region II of a light tank ends at aspect ratios below those of built towers, and anchor reinforcement becomes the normal outcome.

### *6.3 Limitations*

The validation compares two models that share the EN 1992-4 resistance and the assumption of unyielding, uniform supports. It therefore validates the demand idealisation, not the resistance; the latter rests on the narrow-member provisions, which the available evidence suggests are conservative [21], and on no tests of anchor groups in pedestals with four close edges at the force levels considered here. Unequal foundation stiffness, dynamic amplification at partial fill, and the pedestal reinforcement that the criterion does not credit can each move a tower near a boundary; they were outside the scope of this paper and are the subject of separate work. Near a boundary, the criterion should be read as indicative. The uncertainty amplification of Eq. (12), 1.07 for RT-S and 1.33 for RT-H, shows that towers close to the onset of uplift are those whose uplift is least reliably predicted.

### *6.4 Use in Design*

Four uses follow. At scheme stage, $\eta$ and $\rho_a$ place a proposed tower on Fig. 4 or on a map such as Fig. 5, and show whether the pedestal should be sized by Eq. (7), anchor reinforcement planned from the outset, or the base width revisited. In checking, Eq. (4) recovers $\eta$ from two reported reactions, so a tower with $\eta > 1 + \rho_a$ and no documented anchor reinforcement can be identified without re-analysis. In analysis, the rigid-group hand check should carry the 8% allowance for multi-leg towers with corner-supported tanks. In detailing, a Region III embedment is set by Eq. (11), so bolt lengths, templates and the arrangement of anchor reinforcement within a congested pedestal should be resolved at design stage.

## *7. CONCLUSIONS*

1. The design uplift at the windward stanchion of an elevated tank tower equals the factored stabilising load per stanchion multiplied by $(\eta - 1)$, where $\eta$ is a demand ratio known at scheme stage and recoverable from two reported reactions.

2. Under the EN 1992-4 narrow-member rule, the breakout resistance of any symmetric bolt group in a square pedestal of side a cannot exceed $(\sqrt{6}/9)k_1\sqrt{f_{ck}}\, a^{1.5}/\gamma_{Mc}$, a bound that contains no bolt property; it is 163.8 kN for a 700 mm C30/37 pedestal in cracked concrete.
3. Concrete-only anchorage ends at $(H/B)_2 = (H/B)_1(1 + \rho_a)$. At $v_b = 40$ m/s this lies between 1.37 and 2.17 for a 15 m tower with a 100 m³ tank on 700 mm pedestals, so typical towers need anchor reinforcement.
4. The closed form matched frame-based classification for 297 of 300 random towers (99.0%); an 8% demand allowance for multi-leg towers with corner-supported tanks removed the only unconservative case.
5. The aspect ratio makes the anchorage critical by raising the demand, not by reducing the resistance; the decision to provide anchor reinforcement can therefore be taken from tank, tower and pedestal dimensions before any analysis.

**Declaration of generative AI and AI-assisted technologies in the writing process**

During the preparation of this work, the author used Claude (Anthropic) to assist with drafting, restructuring the thesis material into article form and implementing the analysis scripts. After using this tool, the author reviewed and edited the content as needed and takes full responsibility for the publication's content.

**CRediT authorship contribution statement**

Conceptualisation, methodology, software, validation, formal analysis, writing – original draft, review and editing

**Declaration of competing interests**

The authors declare that they have no known competing financial interests or personal relationships that could have appeared to influence the work reported in this paper.

**Funding**

This research received no specific grant from funding agencies in the public, commercial, or not-for-profit sectors.

**Data availability**

The analysis scripts and generated data (Python; seed 20260925 for the random sample) are available.

**Ethical Approval**

Not applicable. This study did not involve human participants or animals.

**Consent to Participate**

Not applicable.

**Consent to Publish**

Not applicable.

**Acknowledgements**
This article is based on typical project work in River State, Nigeria. The design case reactions in Section 3.4 are published with the client's permission.

**Data Availability**
The datasets generated during and/or analyzed during the current study are available from the corresponding author on reasonable request.

**References**

[1] CEN, EN 1992-4:2018 Eurocode 2: Design of concrete structures, Part 4: Design of fastenings for use in concrete, European Committee for Standardization, Brussels, 2018.

[2] ACI Committee 318, Building Code Requirements for Structural Concrete (ACI 318-19) and Commentary (ACI 318R-19), American Concrete Institute, Farmington Hills, MI, 2019.

[3] CEN, EN 1990:2002 Eurocode: Basis of structural design, European Committee for Standardization, Brussels, 2002.

[4] CEN, EN 1991-1-4:2005 Eurocode 1: Actions on structures, Part 1-4: General actions, Wind actions, European Committee for Standardization, Brussels, 2005.

[5] CEN, EN 1993-3-1:2006 Eurocode 3: Design of steel structures, Part 3-1: Towers, masts and chimneys, Towers and masts, European Committee for Standardization, Brussels, 2006.

[6] J.M. Fisher, L.A. Kloiber, Base Plate and Anchor Rod Design, 2nd ed., Steel Design Guide 1, American Institute of Steel Construction, Chicago, 2006.

[7] Q. Zhou, H. Zhang, B. Ma, Y. Huang, Wind loads on transmission tower bodies under skew winds with both yaw and tilt angles, Journal of Wind Engineering and Industrial Aerodynamics 187 (2019) 48–60. https://doi.org/10.1016/j.jweia.2019.01.013

[8] D. Zhang, X. Song, H. Deng, X. Hu, X. Ma, Experimental and numerical study on the aerodynamic characteristics of steel tubular transmission tower bodies under skew

winds, Journal of Wind Engineering and Industrial Aerodynamics 214 (2021) 104678. https://doi.org/10.1016/j.jweia.2021.104678

[9] Y. Tang, Z. Duan, F. Xu, G. Yan, M. Nie, X. Luo, X. Liu, Evaluation of wind loads on square transmission towers with angle members under skewed winds, Journal of Wind Engineering and Industrial Aerodynamics 229 (2022) 105134. https://doi.org/10.1016/j.jweia.2022.105134

[10] W. Zhang, Y. Xiao, C. Li, Q. Zheng, Y. Tang, Wind load investigation of self-supported lattice transmission tower based on wind tunnel tests, Engineering Structures 252 (2022) 113575. https://doi.org/10.1016/j.engstruct.2021.113575

[11] A.B. Jeddi, Z. Azzi, A. Shafieezadeh, A. Elawady, A. Gan Chowdhury, P. Irwin, Revisit of underestimated wind drag coefficients and gust response factors of lattice transmission towers based on aeroelastic wind tunnel testing and multi-sensor data fusion, Engineering Structures 278 (2023) 115486. https://doi.org/10.1016/j.engstruct.2022.115486

[12] Z. Azzi, A. Elawady, P. Irwin, A. Gan Chowdhury, C. Abi Shdid, Aeroelastic modeling to study the wind-induced response of a self-supported lattice tower, Engineering Structures 245 (2021) 112885. https://doi.org/10.1016/j.engstruct.2021.112885

[13] W. Hu, H. Bohra, E. Azzuni, S. Guzey, The uplift effect of bottom plate of aboveground storage tanks subjected to wind loading, Thin-Walled Structures 144 (2019) 106241. https://doi.org/10.1016/j.tws.2019.106241

[14] Y.-C. Chiang, S. Guzey, Dynamic analysis of aboveground open-top steel tanks subjected to wind loading, Engineering Structures 198 (2019) 109496. https://doi.org/10.1016/j.engstruct.2019.109496

[15] A.M. Mansour, M.M. Kassem, F. Mohamed Nazri, Seismic vulnerability assessment of elevated water tanks with variable staging pattern incorporating the fluid-structure interaction, Structures 34 (2021) 61–77. https://doi.org/10.1016/j.istruc.2021.07.062

[16] H. Rimal, P. Pradhan, D. Gautam, R. Rupakhety, Seismic fragility of aging elevated water tank with smooth bars considering soil structure interaction, Buildings 13 (2023) 4. https://doi.org/10.3390/buildings13010004

[17] H. Alemzadeh, H. Shakib, M. Khanmohammadi, Development of rocking isolation for response mitigation of elevated water tanks under seismic and wind hazards, Shock and Vibration 2020 (2020) 5498298. https://doi.org/10.1155/2020/5498298

[18] H. Hammoum, K. Bouzelha, Y. Sellam, L. Haddad, Structural reliability of elevated water reservoirs under wind loading, Procedia Structural Integrity 22 (2019) 235–242. https://doi.org/10.1016/j.prostr.2020.01.030

[19] W. Fuchs, R. Eligehausen, J.E. Breen, Concrete capacity design (CCD) approach for fastening to concrete, ACI Struct. J. 92 (1995) 73–94.

[20] R. Eligehausen, R. Mallée, J.F. Silva, Anchorage in Concrete Construction, Ernst & Sohn, Berlin, 2006.

[21] E.J. Stehle, A. Sharma, Concrete breakout capacity of tension-loaded fastenings in narrow concrete members, Structural Concrete 27 (2026) 6014–6031. https://doi.org/10.1002/suco.70481

[22] T. Karmokar, A. Mohyeddin, J. Lee, T. Paraskeva, Concrete cone failure of single cast-in anchors under tensile loading: A literature review, Engineering Structures 243 (2021) 112615. https://doi.org/10.1016/j.engstruct.2021.112615

[23] Z. Qian, X. Lu, M. Sheng, Experimental investigation of the tensile capacity for anchor groups with different spacing between cast-in-place headed anchors of high strength

and deep embedment, Arabian Journal for Science and Engineering 44 (2019) 4745–4755. https://doi.org/10.1007/s13369-018-3548-9

[24] B. Bokor, A. Sharma, T. Pregartner, An assessment method to ensure applicability of concrete capacity method for design of anchorages: Linear force distribution approach, Structural Concrete 24 (2023) 1-23. https://doi.org/10.1002/suco.202300255

[25] A. Sharma, R. Eligehausen, A new design model for anchorages with flexible elastic base plate for concrete breakout failure under tension loads, Structural Concrete 26 (2025) 4365–4388. https://doi.org/10.1002/suco.202401139

[26] D.A. Grilli, A.M. Kanvinde, Tensile strength of embedded anchor groups: Tests and strength models, Eng. J. (AISC) 53 (2016) 87–98. https://doi.org/10.62913/engj.v53i2.1097

[27] S. Kishiki, X. Yang, T. Ishida, N. Tatsumi, S. Yamada, Experimental study of concrete breakout failure mechanism in an exposed column base with a foundation beam, Engineering Structures 243 (2021) 112661. https://doi.org/10.1016/j.engstruct.2021.112661

[28] B.L. Worsfold, J.P. Moehle, Shear-reinforced concrete breakout design methodology for moment transfer at column-foundation connections, Engineering Structures 283 (2023) 115783. https://doi.org/10.1016/j.engstruct.2023.115783

[29] D. Petersen, Z. Lin, J. Zhao, Design of anchor reinforcement for seismic tension loads, Engineering Structures 164 (2018) 109–118. https://doi.org/10.1016/j.engstruct.2018.02.015

[30] N. Vita, A. Sharma, J. Hofmann, Bonded anchors with post-installed supplementary reinforcement under tension loading: Experimental investigations, Engineering Structures 252 (2022) 113754. https://doi.org/10.1016/j.engstruct.2021.113754

[31] Y. Xu, C. Chen, M. Xie, J. Gong, Experimental study of the influence of supplementary reinforcement on tensile breakout capacity of headed anchors in nuclear power plant equipment foundations, Buildings 14 (2024) 3027. https://doi.org/10.3390/buildings14093027

[32] D. Suthar, A. Sharma, R. Piccinin, B. Bokor, Experimental investigation on post-installed anchorages with cast-in anchor reinforcement under tension loading, Structural Concrete 27 (2026) 6156–6175. https://doi.org/10.1002/suco.70478

[33] ASCE, Minimum Design Loads and Associated Criteria for Buildings and Other Structures (ASCE/SEI 7-22), American Society of Civil Engineers, Reston, VA, 2022.